THEORETICAL CALCULATION OF THE LIQUID-VAPOR COEXISTENCE CURVE OF WATER, CHLOROFORM AND METHANOL WITH THECAVITY-BIASED MONTE CARLO METHOD IN THE GIBBS ENSEMBLE

MIHALY MEZEI

Department of Physiology and Biophysics, Mount Sinai School of Medicine, CUNY. New York, NY 10029

The Gibbs ensemble computer simulation method of Panagiotopoulos is combined by the cavity-biased sampling technique used previously in the grand-canonical ensemble. The combined technique is applied to the determination of the liquid-vapor coexistence curve of the Lennard Jones fluid as a test case, two water models (SPC and TIP4P) as well as methanol and chloroform, both described with the OPLS model. The application of the virial-biased sampling technique, used earlier in the isobaric ensemble is also discussed.

KEY WORDS: Gibbs ensemble, liquid-vapor coexistence, water, methanol, chloroform.

INTRODUCTION

The liquid-vapor coexistence curve for any type of particles can in general be calculated if both the free energy and the presure of the liquid and the gas is known as a function of the density and the temperature. For the Lennard-Jones fluid, such an equation of state has been determined using extensive data from several different authors [1]. Alternatively, a number of free energy calculations can be performed to find out the conditions under which the liquid and vapor free energies and pressures agree. Again, these calculations are known to be computationally rather expensive [2]. Panagiotopoulos recently proposed what he called the Gibbs ensemble [3,4], involving a dual simulation of two systems — one of them is the liquid the other is the vapor — that exchange both volume and matter to reach equilibrium between the two. The two systems are not in physical contact, thus problems that arise with modeling the liquid-vapor interface are avoided. This technique has been verified on the well-characterized liquid vapor coexistence curve of the Lennard-Jones fluid [3]. Subsequent work has been reviewed by Panagiotopoulos [5]. As the method requires insertions into both

systems, the first applications to liquid water were done above room temperature [6]. Room temperature calculations require specialized techniques, as discussed below.

The recent success of the cavity-biased insertions in the grand-canonical ensemble [7,8] suggests that an generalization of this technique to the Gibbs ensemble would extend the temperature range where simulations can be done. This suggesion is tested in the present study. As remarked in Ref.8, the success of the insertion of an anisotropic molecule can be enhanced by the use of an orientational bias. Cracknell, Nicholson, Parsonage and Evans recently developed a procedure for orientationally biased insertion and tested it in the Gibbs ensemble [9] and the success of exchanges was indeed found to improve significantly. It is thus expected that the combination of the cavity biased insertion with the orientationally biased insertion should prove even more powerful since they are each helpful under different circumstances. In addition to the cavity-biased insertion technique, it is likely that the volume change can also be made more efficient by implementing the virial-biased technique [10]. This paper describes the generalization of the cavity-biased insertion technique and the virial-biased volume change technique to Gibbs ensemble simulations and presents results on water, methanol and chloroform using the cavity biased technique. Comparison with other methods as well as with experimental results will also be presented.

BACKGROUND

Gibbs ensemble simulation

Simulation in the Gibbs ensemble combines simulation techniques in the canonical, isobaric and grand-canonical ensembles (all at constant temperature). It proposes the dual simulations of the substance under consideration in two different phases. The particles in both of the systems are moved independently of each other but the volume changes and the particle number changes are correlated: volumes and particles are only exchanged between the two systems, i.e., a volume change involves the change in the two volumes by the same amount ΔV but in different directions and the disappearence of a particle from one system can only occur with an insertion of a new particle into the other system. If one combines the probability ratios of the simultaneous changes, both the pressure and the chemical potential cancels and one is left with acceptance expressions that involve only the volumes, particle numbers, energies and the temperature:

$$P_{\text{vol}} = \exp[(\Delta E^a + \Delta E^b)/kT][(V^a + \Delta V)/V^a]^{N^a}[(V^b - \Delta V)/V^b]^{N^b} \qquad (1)$$

$$P_{\text{int}} = \exp[(\Delta E^a + \Delta E^b)/kT]V^b(N^a + 1)/(V^a N^b) \qquad (2)$$

where k is the Boltzmann constant, T is the absolute temperature, the superscripts a and b refer to the two systems, respectively, E is the internal energy, N is the number of particles and V is the volume. By performing Gibbs ensemble simulations at various temperatures the coexistence curve of the two phases can be determined.

The outcome of a simulation with this technique will be average internal energies and the densities of two systems at equilibrium, at the temperature specified by T. With some extra

computational effort the pressures in the two systems can also be estimated and their difference could provide an estimate of the precision of the simulation. The extra computational effort becomes minimal when the force-biased displacement technique of Rao, Pangali and Berne [11] is used or for atomic fluids described by inverse distance power potentials [12].

Cavity-biased Gibbs ensemble simulation

As one of the computational steps in the Gibbs ensemble is essentially a grand-canonical ensemble insertion and deletion, the difficulties encountered at high densities in the grand-canonical ensemble will be encountered in the Gibbs ensemble as well. However, techniques overcoming that difficulty should be equally applicable.

Recently, it has been shown that using a cavity-biased insertion technique [8] liquid water can successfully be simulated in the grand-canonical ensemble. The cavity biased method inserts only into cavities of suitable size (e.g., with radius greater than R_c). The probabilities of the acceptance of a cavity-biased insertion is

$$P_{CB}^{i} = V' P_c^N(\mathbf{r}^N) \exp[(\mu + E(\mathbf{r}^N) - E(\mathbf{r}^{N-1}))/kT]/(N+1). \tag{3}$$

Here μ is the chemical potential, $V' = V\Lambda^3$, where Λ is the usual kinetic factor, $U(\mathbf{r}^N)$ is the potential energy of a system of N particles at the configuration $\mathbf{r}^N$ and $P_c^N(\mathbf{r}^N)$ is the probability of finding a cavity of radius R_c or larger in the configuration $\mathbf{r}^N$. The particle to be deleted is chosen randomly and the corresponding acceptance probability is

$$P_{CB}^{d} = N \exp[(-\mu + E(\mathbf{r}^N) - E(\mathbf{r}^{N-1}))/kT]/(V' P_c^{N-1}(\mathbf{r}^{N-1})). \tag{4}$$

It is easy to show (following the derivation in Reference [4]) that for a cavity biased exchange

$$P_{int}^{CB} = P_{int} P_c^{N^a}/P_c^{N^b} \tag{5}$$

where the particle was transferred from system b to system a.

The probability of finding a cavity at a given point in a given configuration can be efficiently estimated by a grid technique described in Reference [8]. It can be also applied in the Gibbs ensemble, with a single provision, related to the accounting for the effects of the volume changes. If one allows the grid to be scaled by the same factor as the the box edge is scaled with the volume change and redefines the cavity definition by replacing the original R_c with a radius that is also scaled along with the grid, then the cavity description will remain unaffected by the volume changes.

Virial–Biased Gibbs ensemble simulation

The virial-biased constant pressure ensemble simulation biases the volume change in the direction of the derivative, F_v, of the exponent in the constant-ensemble Boltzmann factor as described in detail in Reference [10]. In particular, the volume change ΔV is sampled from the distribution

$$\exp[\lambda \Delta V F_v/kT]/n(V) \tag{6}$$

where

$$F_v = -\partial(U + PV - kTN\ln V)/\partial V, \tag{7}$$

λ is a constant usually chosen to be $1/2$, and

$$n(V) = 2kT\sinh(\lambda\delta V F_v/kT)F_v \tag{8}$$

with δV being the maximum volume change allowed. For systems with pairwise additive potentials $u(\mathbf{r}_1, \mathbf{r}_2)$, used with a spherical cutoff of R_e,

$$F_v = \left[\sum_{i<j}^{N}(\mathbf{r}_i - \mathbf{r}_j)\Delta_i u(\mathbf{r}_i, \mathbf{r}_j)\right]/3V - 2\pi\rho u(R_e)g(R_e)/3 - V + kTN/V. \tag{9}$$

If the potential is smoothly switched to zero ('feathering'), the second term, containing $g(R_e)$, the value of the radial distribution function at the cutoff, is omitted. Note, that the first term was incorrectly given (but correctly used) in Reference [10].

If the volume changes were uncorrelated, the virial-biased technique would be applicable without change in the Gibbs ensemble simulation. This correlation can be incorporated into the biasing process if, for the purpose of the volume change, one considers the two system a single combined system with a single, combined volume change. For this combined volume change the appropriate F_v to be used in Equation (6) is simply

$$F_{\mathrm{v}} = F_{\mathrm{v}}^a - F_{\mathrm{v}}^b. \tag{10}$$

The calculation of F_v, requires the derivative of the energy with respect to the volume. For atomic fluids with inverse distance power potentials, F_{v} can be obtained at negligible computational expense [12]. However, if the pressures of the two fluids are also estimated or if the force-biased technique [11] is used for displacement then the calculation of F_v again requires little extra effort. This technique, however, was not implemented in the work reported here.

CALCULATIONS

In all calculations described here the particles were moved by the Metropolis prescription. The calculations involving molecular fluids also calculated the center of mass **CRM** of each particle. Rotations during the normal Metropolis move were performed around the center of mass of each molecule and a volume change ΔV changed the coordinates of each molecule $\mathbf{X}^i$

$$\mathbf{X}^i_{\mathrm{new}} = \mathbf{X}^i_{\mathrm{old}} + \mathbf{CRM}^i(r_{\mathrm{new}} - r_{\mathrm{old}}) \tag{11}$$

where

$$r = (V/V_{\mathrm{init}})^{1/3}. \tag{12}$$

This way the **CRM** coordinates always refer to the initial volume, V_{init} and the volume change only affects the atomic coordinates **X**. The calculations related to cavity search also use **CRM** to avoid the need for reinitializing the cavity grid each time the volumes are changed.

TABLE 1 Potential parameters used in the calculations.

	σ	ϵ	*Charge*	R_e
TIP4P water O	3.1536	0.15504	-1.04	7.75
TIP4P water H				
TIP4P water q			0.52	
SPC water O	3.1655	0.15542	-0.82	7.75
SPC water H			0.41	
methanol CH_3	3.774	0.207	0.265	9.5
methanol O	3.07	0.168	-0.7	
methanol H			0.435	
chloroform CH	3.8	0.08	0.42	12.0
chloroform Cl	3.47	0.40	-0.14	

Legend: The Lennard-Jones parameters σ and ϵ are in Å and kcal/mol, the charge is in electrons ($E_{\mathrm{LJ}}(r) = 4\epsilon[(\sigma/r)^{12} - (\sigma/r)^6]$) and the potential cutoff R_e is in Å

TABLE 2 Gibbs ensemble simulation results on the Lennard Jones fluid.

T^*	ρ_l	ρ_v	*Ins.*	PX_{acc}	ΔN	*Eq. of state*	
						ρ_l	ρ_v
0.7	0.841±.003	0.0015±.00003	CB	0.0016	4	0.84	0.002
0.7	0.839±.0.001	0.0017±.0007		0.0001	3	0.84	0.002
0.8	0.798±.003	0.0059±.0006	CB	0.0091	7	0.80	0.005
0.8	0.801±.02	0.0073±.003		0.0006	8	0.80	0.005
0.9	0.755±.005	0.014 ±.0011	CB	0.026	14	0.76	0.011
0.9	0.756±.007	0.014 ±.0022		0.0024	11	0.76	0.011
1.0	0.704±.005	0.030 ±.0011	CB	0.057	23	0.70	0.024
1.0	0.697±.010	0.028 ± 0031		0.008	22	0.70	0.024
1.1	0.639±.018	0.052 ±.0059	CB	0.116	41	0.63	0.045
1.1	0.642±.012	0.055 ± .0051		0.017	30	0.63	0.045

Legend: a) Ins. gives the insertion technique; b) PX_{acc} is the acceptance rate of the particle exchange step; c) ΔN is the range of fluctuations in the particle number; d) the density is the reduced density.

TABLE 3 Gibbs ensemble simulation results on the SPC water.

T	ρ_l	ρ_v	Ins.	PX_{acc}	ΔN	N_{MC}	Experimental	
							ρ_l	ρ_v
298	1.009±.007	0.00008±0.0002	CB	0.00007	1	1000K	0.998	0.00002
350	0.952±.011	0.00025±0.0001	CB	0.0007	3	1000K	0.983	0.00015
400	0.879±.010	0.0014 ±0.0002	CB	0.0045	3	1000K	0.951	0.00088
450	0.826±.011	0.0069 ±0.0012	CB	0.014	9	1000K	0.908	0.0032
500	0.717±.020	0.0182 ±0.0026	CB	0.034	19	1000K	0.853	0.0097
550	0.604±.027	0.063 ±0.018	CB	0.050	54	1000K	0.786	0.0234
570	0.557±.056	0.152 ±0.033	CB	0.037	78	850K	0.749	0.0349
580	0.396±.147	0.324 ±0.045	R	0.050	154	1000K	0.731	0.0407

Legend: a) *Ins.* gives the insertion technique; b) PX_{acc} is the acceptance rate of the particle exchange step; c) ΔN is the range of fluctuations in the particle number; d) the density is in g/ml; e) experimental data interpolated from Reference [25].

The Lennard-Jones calculations used 165 particles and the molecular systems contained 190 molecules. Exchange attempts were made after every displacement attempts of a randomly selected particle in both systems, and the direction of the exchage attempts was alternated. Volume change attempts were performed after every 100 displacement and exchange attempts. No optimization of these parameters was performed. Note, that Cracknell *et al.* found better results with less frequent exchange attempts [9].

As all the calculations described here deal with liquid-vapor coexistence curves, the cavity-biased insertion was only applied to the liquid system. The generation of initial configurations reflected this requirements: at first (T, V, N) ensemble calculations equilibrated a single liquid system at the temperature of the calculation with the density targeted and only after this equilibration was the Gibbs ensemble calculation started.

Each calculation used a spherical cutoff on the interactions (based on the distances of the center of masses), given in Table 1. Unlike the cavity radius, the cutoff radius was not scaled with the volume change. This introduced the possibility that the volume of a system could drop below the minimum volume required to contain the cutoff sphere. Clearly, this should be avoided since it would bias uncontrollably the volume sampling. In the present implementation the calculation was stopped if that occurred and additional particles were added.

The calculations on the Lennard Jones fluid, run with a 2.5σ cutoff, used a correction for the contributions beyond the cutoff distance to allow comparison with published results. The correction is based on the assumption that the radial distribution function is constant beyond the cutoff distance R_e. This procedure is less involved than the one used in Reference [3],

but it was found to be adequate earlier for the Lennard Jones fluid [13]. The contribution (in reduced units) is

$$(N/2) \int_0^\infty (4\pi r^2 \rho)[4(r^{-12} - r^{-6})]\mathrm{dr} = (R_e^{-9}/9 - R_e^{-3}/3)8\pi N^2/V. \qquad (13)$$

The value of this expression changes both on the interchage of particles and on the exchange of volumes and therefore the acceptance probabilities of both of those steps have to be modified accordingly.

The errors on the calculated average volumes $\langle V \rangle$ and number of particles $\langle N \rangle$ were calculated by the method of batch means [14,15] and the errors on the densities were obtained by assuming that the relative error on the density is the sum of the relative errors of $\langle V \rangle$ and of $\langle N \rangle$. The numbers given are the doubles of the standard deviations and thus represent 95% confidence interval.

The location of the critical point was estimated by fitting a third order polynomial to the nearest 5 (two sets) and 6 points to the critical point and averaging the estimates from these fits.

The calculations on liquid water were based on the TIP4P [16] and the SPC [17] water models. The OPLS parameters for methanol are given in References [18] and [19] while the chloroform parameters are in Reference [20]. Table 1 collects the potential parameter values used.

RESULTS AND DISCUSSION

Table 2 shows the results of calculations on Lennard-Jones particles run at various temperatures and their comparison with previous results. The calculations were run both with random insertions and with the cavity bias insertions. The cavity-biased technique increased the acceptance rate of the exchange step by an order of magnitude and, with the exception of the $T^* = 1.1$ run (where the random insertion was already producing nearly 2% acceptance rate), the error on the calculated density was also significantly reduced.

The calculations on the SPC water, using a 7.75 Å spherical cutoff (SC) are described in Table 3. Figure 1 gives a comparison with the calculations of de Pablo *et al.* [21] where the Ewald summation (ES) was employed instead of SC and with the exmerimental liquid and vapor densities. The liquid densities calculated with the SC boundary conditions are closer to the experimental values than the ES results under the critical point but the calculated critical temperature is similar for both boundary conditions, 587 K for ES and 582 K for SC (and thus both significantly under the experimental value, 647.3 K) and the calculated critical densities, 0.38 g/ml for SC and 0.27 g/ml for ES, differ from the experimental value, 0.32 g/ml by the same amount although in different directions. The better behaviour of the SC calculation near room temperature is not surprising since the SPC potential was parametrized with SC. Reparametrization with ES based on room temperature data, however, would likely to worsen the calculated critical density although the calculated critical temperature might

improve. In hindsight, one might also argue that unless it is ensured that the simulation cell sizes are (nearly) constant over the temperature range studied, using ES in Gibbs ensemble simulations introduces an inconsistency and that is manifested in the weaker comparison with experiment. Clearly, more studies are required on this point.

The results of the methanol and chloroform calculations are given in Tables 3 and 4, respectively. The agreement with experiment for methanol is rather good until 450 K and again at the critical point calculated to be at 0.25 g/ml and 493 K, close to the experimental result, 0.2722 g/ml and 513.2 K [22]. The comparison for chloroform shows similar behaviour. Its critical point was found to be at 0.63 g/ml and 504 K. This differs somewhat more from the experimental value, 0.516 g/ml and 536.1 K [22] or 0.491 g/ml and 536.7 K [23].

TABLE 4 Gibbs ensemble simulation results on the OPLS methanol.

T	ρ_l	ρ_v	Ins.	PX_{acc}	ΔN	N_{MC}	Experimental	
							ρ_l	ρ_v
275	0.777±.006	0.00908±0.0006	CB	0.00002	2	1000K	0.808	0.00007
298	0.744±.013	0.00238±0.0024	CB	0.0009	9	1000K	0.787	0.00022
350	0.693±.011	0.0055 ±0.0024	CB	0.0052	12	1000K	0.739	0.0019
400	0.630±.022	0.0208 ±0.0045	CB	0.015	23	1000K	0.681	0.0087
450	0.537±.067	0.111 ±0.021	CB	0.023	71	1000K	0.604	0.0297
480	0.313±.067	0.181 ±0.075	R	0.043	165	1000K	0.534	0.0605
490	0.291±.059	0.238 ±0.029	R	0.039	90	1000K	0.501	0.0795
500	0.254±.039	0.261 ±0.060	R	0.046	65	1000K	0.478	0.107

Legend: a) Ins. gives the insertion technique; b) PX_{acc} is the acceptance rate of the particle exchange step; c) ΔN is the range of fluctuations in the particle number; d) the density is in g/ml. Experimental data interpolated from References [22] and [25].

For the comparison with experimental thermodynamic properties, however, it should be borne in mind that the potentials used in this work are all effective pairwise additive potentials that have been parametrized to data near room-temperature. The range of applicability of such potentials is in general limited to thermodynamic states that sample the same region of the configuration space. It is clearly unreasonable to expect that this would be the case for the triple point and the critical point of a liquid. Thus extending the use of an effective pair potential derived around room temperature to the critical point means 'pushing' it beyond its range of applicability and thus significant degradation in performance is likely to occur. If better modeling of liquids near the critical point is required, there are two options: reparametrize the potential as a function of temperature or turn to the use of cooperative potentials. Recent calculations of Strauch and Cummings, that used different dipole monents in different phases and obtained improved agreement with experiment [24], fall into the first category.

The introduction of the cavity-biased insertion increased the computer time by 35% for the Lennard-Jones system. In exchange, it increased the acceptance rate by an order of magnitude for the Lennard Jones fluid, and concomittantly reduced the error on the densities by a factor of two or more. Such reduction of error is approximately equivalent to lengthening the run to four times longer or more.

TABLE 5 Gibbs ensemble simulation results on the OPLS chloroform..

T	ρ_l	ρ_v	Ins.	PX_{acc}	ΔN	N_{MC}	Experimental	
							ρ_l	ρ_v
298	1.452±.014	0.00060±0.00087	CB	0.00001	1	1000K	1.481	
350	1.349±.021	0.0162 ±0.0068	CB	0.00029	6	1000K	1.417	0.0046
400	1.240±.013	0.0292 ±0.0046	CB	0.0032	10	1000K	1.375	0.0197
450	1.105±.023	0.0794 ±0.011	R	0.0049	32	1000K	1.254	0.0503
500	0.860±.101	0.632 ±0.142	R	0.015	90	1000K	1.097	0.117
510	0.796±.134	0.742 ±0.134	R	0.015	94	1500K	1.057	0.138
520	0.772±.154	0.772 ±0.156	R	0.016	109	1500K	1.014	0.165

Legend: a) Ins. gives the insertion technique; b) PX_{acc} is the acceptance rate of the particle exchange step; c) ΔN is the range of fluctuations in the particle number; d) the density is in g/ml; e) experimental data interpolated from Reference [23].

To estimate the effect of the cavity-biased insertions, calculations were also done on the molecular systems at room temperature using random insertion attempts. The acceptance of the exchange steps at 298K increased by a factor of 4, 8, 5, and 2.5 for the TIP4P water, SPC water, methanol and chloroform, respectively, while the computer time increase by 21% for the SPC water, 16% for the TIP4P water, 10% for methanol, and 9% for chloroform. Thus the suggestion of Cracknell et al. [9] that cavity biasing would be of little importance for water is not supported by this work.

The fluctuation in the liquid volumes resulted in samll fluctuation on the cavity radius R_c. The average cavity radius differed from the cavity radius at the initial configuration by at most 1%, 2%, and 8% for the water, chloroform and methanol systems, respectively. As the calculation is relatively insensitive to the precise value of R_c, the decision to allow R_c to fluctuate with V is justified.
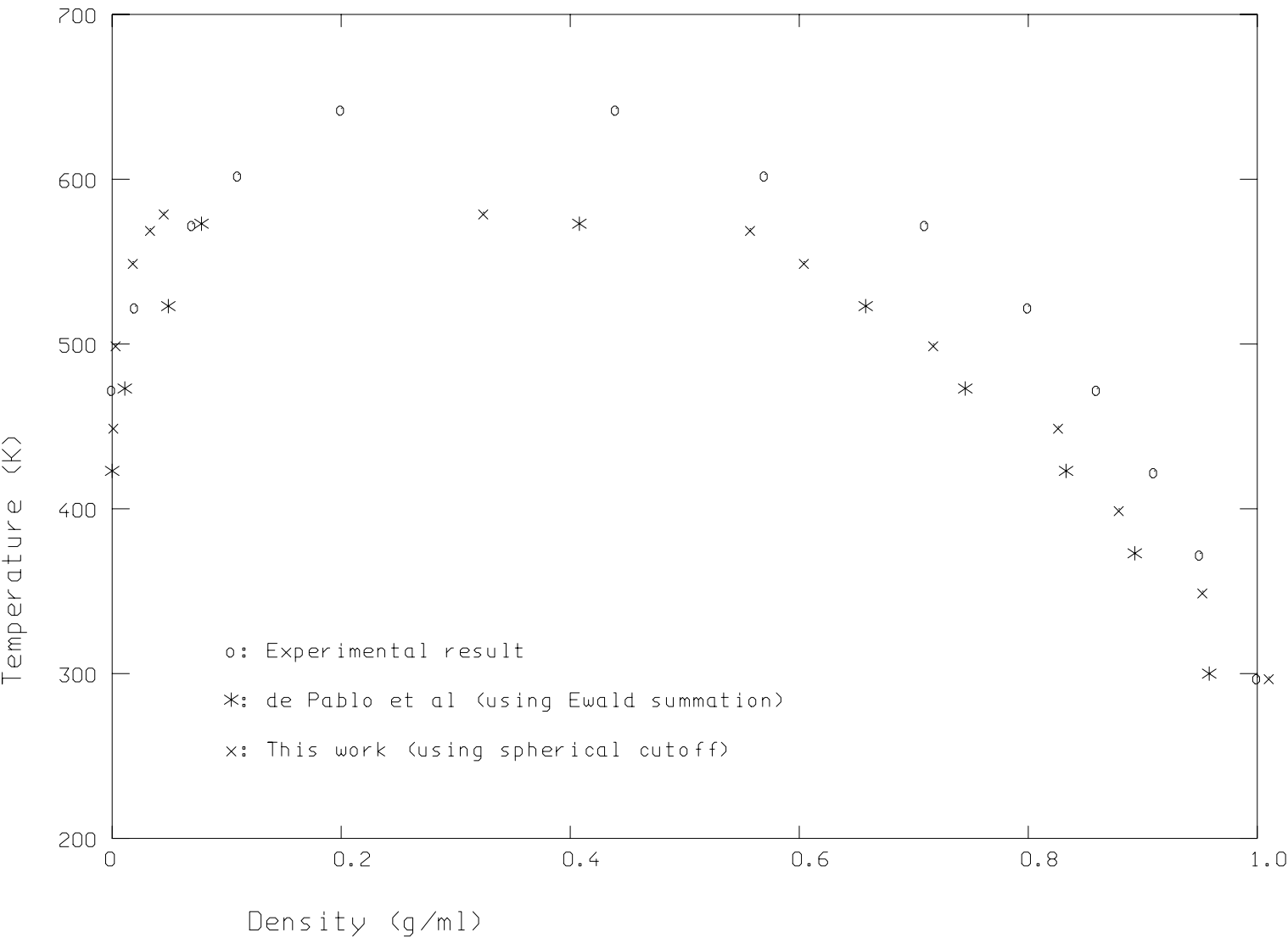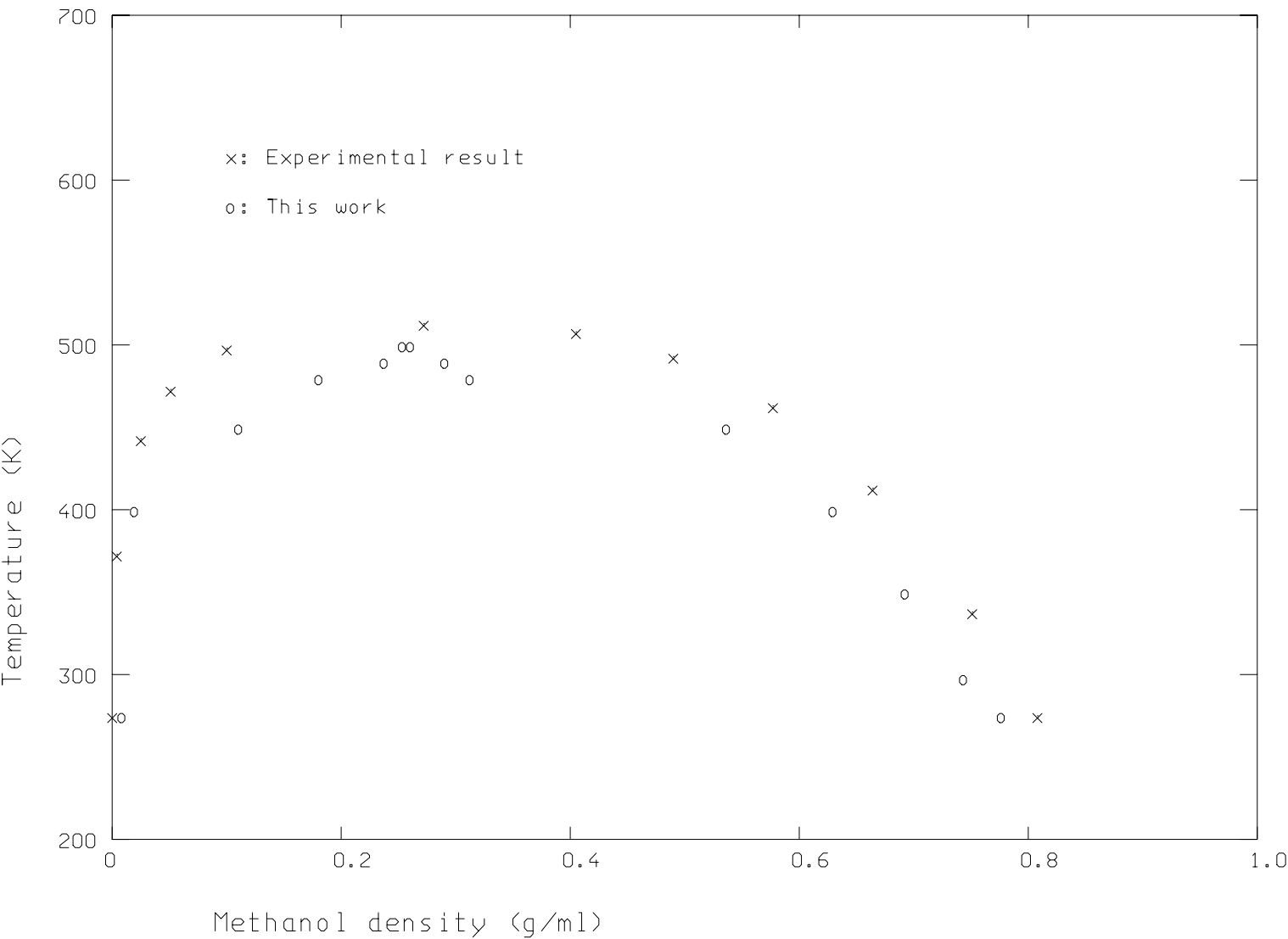
References.

[1] J.J. Nicolas, K.E Gubbins, W.B. Street and D.J. Tildesley, "Equation of state for the Lennard Jones fluid," *Molec. Phys.*, **37**, 1429 (1979).

[2] M. Mezei and D.L. Beveridge, "Free energy simulations," *Ann. Acad. Sci. N.Y.*, **482**, 1 (1986).

[3] A.Z. Panagiotopoulos, "Direc determination of phase coexistence properties of fluids by Monte Carlo simulation in a new ensemble," *Molec. Phys.*, **61**, 813 (1987).

[4] A.Z. Panagiotopoulos, N. Quirke, M. Stapleton and D.J. Tildesley, "Phase equilibria by simulation in the Gibbs ensemble: alternative derivation, generalization and application to mixture and membrane equilibria," *Molec. Phys.*, **63**, 527 (1988).

[5] A.Z. Panagiotopoulos, "Direct determination of fluid phase equilibria by simulation in the Gibbs ensemble: a review," *Molecular Simulation*, in press.

[6] J.J. De Pablo and J.M. Prausnitz, "Phase equilibria for fluid mixtures from Monte Carlo simulations," *Fluid Phase Equil.*, **56**, 177 (1989).

[7] M. Mezei, "A cavity-biased (T,V,μ) Monte Carlo method for the computer simulation of fluids." *Molec. Phys.* **40**, 901 (1980).

[8] M. Mezei, "Grand-canonical ensemble Monte Carlo study of dense liquids: Lennard-Jones, soft spheres and water," *Molec. Phys.* **61**, 565 (1987); erratum: **67**, 1207 (1989).

[9] R.F. Cracknell, D. Nicholson and N.G. Parsonage, "Rotational inserton bias: a novel method for calculating phase equilibria," *Mol. Phys.*, **71**, 931 (1990).

[10] M. Mezei, "Virial-bias Monte Carlo methods. Efficient sampling in the (T,P,N) ensemble," *Molec. Phys.* **48**, 1075 (1983).

[11] M. Rao, C.S. Pangali and B.J. Berne, "On the force Bias Monte Carlo simulation of water: Methodology, optimization and comparison with molecular dynamics," *Molec. Phys.*, **37**, 1779 (1979).

[12] M. Mezei, "The possibility of obtaining an effective pairwise additive intermolecular potential via an ab initio route by fitting to a cooperative model of condensed-phase configurations," *J. Phys. Chem.*, **95**, 7042 (1991).

[13] M. Mezei, "Direct calculation of the excess free energy of the dense Lennard-Jones fluid", *Molecular Simulation*, **2**, 201 (1989).

[14] W.L. Jorgensen, J. Chandrashekar, J.D. Madura, R. Impey and M. Klein, "Comparisons of simple potential functions for simulating liquid water," *J. Chem. Phys.*, **79**, 926 (1983).

[15] R.B. Blackman, and J.W. Tuckey, "The Measurement of Power Spectra," Dover (1958).

[16] "Monte Carlo studies of simple liquid models," in *Physics of Simple Liquids,* H.N.V. Temperley, J.S. Rowlinson, and G.S. Rushbrooke, eds., North Holland, (1968).

[17] H.J.C. Berendsen, J.P.M. Postma, W.F. van Gunsteren and J. Hermans, in "Intermolecular Forces", B. Pullman, ed., Reidel (1981).

[18] W.L. Jorgensen, "Optimized intermolecular potential functions for liquid alcohols," *J. Phys. Chem.*, **90**, 1276 (1986).

[19] W.L. Jorgensen, J.D. Madura and C. Swenson, "Optimized intermolecular potential functions for liquid hydrocarbons," *J. Am. Chem. Soc.*, **106**, 6638 (1984).

[20] W.L. Jorgensen, J.M. Briggs and M.L. Contreras, "Relative partition coefficient for organic solutes from fluid simulations," *J. Phys. Chem.*, **94**, 1683 (1990).

[21] J.J. de Pablo, J.M. Prausnitz, H.J. Strauch and P.T. Cummings, "Molecular simulation of water along the liquid-vapor coexistence curve from 25°C to the critical point," *J. Chem. Phys.*, **93**, 7355 (1990).

[22] "International Critical Tables,", Vol 3, McGraw Hill, New York (1928).

[23] "The critical constants and orthobaric densities of acetone, chloroform, benzene and carbon tetrachloride," *Can. J. Chem.*, **47**, 3893 (1969).

[24] "Comment on: Molecular Simulation of water along the liquidvapor coexistence curve from 25°C to the critical point," *J. Chem. Phys.*, **96**, 864 (1992).

[25] "Perry's Chemical Engineers' Handbook", 6th Ed., R.H. Perry, D.W. Greed, eds., McGraw Hill, New York (1984).

Liquid-vapor coexistence curve for SPC water

o: Experimental result

*: de Pablo et al (using Ewald summation)

x: This work (using spherical cutoff)

Liquid-vapor coexistence curve for OPLS methanol

Liquid-vapor coexistence curve for OPLS chloroform

x: Experimental result

o: This work

Temperature (K)

Chloroform density (g/ml)